Epithelial Progeny of Estrogen-Exposed Breast Progenitor Cells Display a Cancer-like Methylome

Alfred S.L. Cheng,[1,6] Aedín C. Culhane,[2] Michael W.Y. Chan,[1,7] Chinnambally R. Venkataramu,[3] Mathias Ehrich,[4] Aejaz Nasir,[3] Benjamin A.T. Rodriguez,[1] Joseph Liu,[1] Pearlly S. Yan,[1] John Quackenbush,[2] Kenneth P. Nephew,[5] Timothy J. Yeatman,[3] and Tim H-M. Huang[1]

[1]Human Cancer Genetics Program, Department of Molecular Virology, Immunology and Medical Genetics, Comprehensive Cancer Center, The Ohio State University, Columbus, Ohio; [2]Department of Biostatistics and Computational Biology, Dana-Farber Cancer Institute, Boston, Massachusetts; [3]Department of Interdisciplinary Oncology, H. Lee Moffitt Cancer Center and Research Institute, Tampa, Florida; [4]Sequenom, Inc., San Diego, California; [5]Medical Sciences, Indiana University School of Medicine, Bloomington, Indiana; [6]Institute of Digestive Disease, The Chinese University of Hong Kong, Hong Kong Special Administrative Region, China; and [7]Department of Life Science and Institute of Molecular Biology, National Chung Cheng University, Taiwan, Republic of China

Abstract

Estrogen imprinting is used to describe a phenomenon in which early developmental exposure to endocrine disruptors increases breast cancer risk later in adult life. We propose that long-lived, self-regenerating stem and progenitor cells are more susceptible to the exposure injury than terminally differentiated epithelial cells in the breast duct. Mammospheres, containing enriched breast progenitors, were used as an exposure system to simulate this imprinting phenomenon *in vitro*. Using MeDIP-chip, a methylation microarray screening method, we found that 0.5% (120 loci) of human CpG islands were hypermethylated in epithelial cells derived from estrogen-exposed progenitors compared with the non–estrogen-exposed control cells. This epigenetic event may lead to progressive silencing of tumor suppressor genes, including *RUNX3*, in these epithelial cells, which also occurred in primary breast tumors. Furthermore, normal tissue in close proximity to the tumor site also displayed *RUNX3* hypermethylation, suggesting that this aberrant event occurs in early breast carcinogenesis. The high prevalence of estrogen-induced epigenetic changes in primary tumors and the surrounding histologically normal tissues provides the first empirical link between estrogen injury of breast stem/progenitor cells and carcinogenesis. This finding also offers a mechanistic explanation as to why a tumor suppressor gene, such as *RUNX3*, can be heritably silenced by epigenetic mechanisms in breast cancer. [Cancer Res 2008;68(6):1786–96]

Introduction

Prolonged exposure to estrogen and related endocrine disruptors during early development increases the risk of developing breast cancer (1, 2). These hormonally active agents have been shown to disrupt normal development of breast epithelia and support the growth of breast tumors (1, 2). Animal and epidemiologic studies suggest an imprinting phenomenon in which early exposure to estrogenic chemicals potentiates a carcinogenic process that is not observed until later in adult life (1, 3). Recent studies imply that estrogen imprinting can be mediated by an epigenetic mechanism (3, 4), a process that influences the phenotypic outcome of a gene without genetic changes of the underlying DNA sequence. DNA methylation, a key epigenetic modification, occurs frequently in CpG islands located near the promoters of silenced genes during disease development (5). Hypermethylation of promoter CpG islands is now considered to be a common mechanism for the heritable maintenance of gene silencing in human cancer (6).

Although developmental exposure to estrogens results in aberrant imprinting and subsequent transformation of breast epithelia (1), the cellular process underlying this phenomenon remains unknown. We hypothesize that breast stem and progenitor cells are primary targets of estrogenic exposure. These slowly dividing cells are capable of self-renewing and, in response to specific signaling, give rise to an amplifying population of progenitors that subsequently differentiate into different epithelial lineages (7). As the property of self-renewal allows for a long life span of stem cells, we speculate that these undifferentiated cells are highly susceptible to environmental injuries over time and transmit their "injury memory" to differentiated progeny through an epigenetic mechanism.

Using a methylation screening method, we report here that epithelial progeny of estrogen-exposed breast progenitors exhibits aberrant patterns of DNA methylation similar to those of known tumor suppressor genes in primary tumors. This cancer-like DNA methylation epigenome, or methylome (8), is associated with abnormal clonal expansion of epithelial progeny. Furthermore, the prevalence of estrogen-induced hypermethylation in tumors and adjacent normal tissues suggests that these epigenetic alterations occur early during breast carcinogenesis.

Materials and Methods

Tissue samples and cell lines. Tissues were collected in accordance with the protocols approved by the Institutional Review Boards of the University of South Florida and the Ohio State University. Breast tissues from patients that underwent mastectomy were collected. Specimens were marked for tumor and in some cases including its four surrounding zones (1, 2, 3, and 4 cm away from the grossly visible tumor boundary; see Fig. 5*A*). Samples from each zone were collected and frozen in liquid nitrogen. In contralateral mastectomy cases, normal tissues were taken from the four quadrants of the breast. Tissues were also obtained from healthy individuals undergoing breast reduction mammoplasty. Frozen tissues mounted on slides were marked and microdissected as described previously (9). Adipose tissues were trimmed away; the tumor and "normal" tissues were separated

Note: Supplementary data for this article are available at Cancer Research Online (http://cancerres.aacrjournals.org/).

M. Ehrich is a shareholder and employee of Sequenom, Inc.

Requests for reprints: Tim H-M. Huang, Human Cancer Genetics Program, Department of Molecular Virology, Immunology and Medical Genetics, Comprehensive Cancer Center, The Ohio State University, Columbus, OH 43210. Phone: 614-688-8277; Fax: 614-292-5995; E-mail: tim.huang@osumc.edu.

doi:10.1158/0008-5472.CAN-07-5547

and stored in liquid nitrogen. Histologic examination of tissue sections and microdissection of samples were conducted in close collaboration with a pathologist to ensure consistency in the clinical diagnoses. Tissues adjacent to tumors were defined to be mostly unremarkable breast ducts or breast with cystic changes, mild ductal hyperplasia, or other nonproliferative changes. DNA was isolated from these samples as described previously (9). Breast cancer cell lines Hs578t, MCF-7, MDA-MB-134, MDA-MB-231, MDA-MB-435s, MDA-MB-453, T47D, and ZR75-1 were obtained from the American Type Culture Collection.

Mammosphere culture and estrogen treatment. Normal breast tissues were obtained from healthy individuals (age range, 15–60 y; average, 34) undergoing reduction mammoplasties mainly due to macromastia. The tissues were dissociated mechanically and enzymatically, and single cells were grown into mammospheres in ultralow attachment plates (Cloning) in serum-free mammary epithelial growth medium (Cambrex) containing 20 ng/mL epidermal growth factor (EGF), 20 ng/mL basic fibroblast growth factor, 1× B27, and 4 μg/mL heparin as described (10). Breast stem/progenitor cells were dissociated from primary mammospheres and treated with 70 nmol/L 17β-estradiol (E2; Sigma) or DMSO in phenol red–free medium for 2 wk (medium changed twice weekly). This estrogen treatment scheme has previously been shown to trigger neoplastic development of normal breast epithelial cells (11). After a 2-wk exposure period, mammosphere-derived cells were cultured on a collagen substratum (BD Biosciences) for an additional 2 to 3 wk. The cells were differentiated into epithelia in estrogen-free conditions using phenol red–free DMEM/F12 medium supplemented with 5% charcoal-dextran–treated fetal bovine serum (FBS; Hyclone), 5 μg/mL insulin, 1 μg/mL hydrocortisone, 10 ng/mL cholera toxin, and 10 ng/mL EGF as described previously (10). Total RNA, isolated from mammospheres and the derived epithelial cells using Trizol (Sigma), was used for real-time quantitative reverse transcription-PCR (RT-PCR) as described previously (12). Specific primers for amplification are available on request. DNA was extracted using QIAamp DNA Mini kit (Qiagen).

Immunofluorescence staining. Two thousand cells dissociated from mammospheres were seeded onto collagen-coated disks (BD Biosciences), placed on 6-cm-diameter dishes, and cultured as described above. Cells were fixed with 4% paraformaldehyde for 10 min and permeabilized with 0.1% Triton X-100 for 10 min. After blocking with 10% normal goat serum (Vector Laboratories) for 30 min, the cells were incubated with antibodies against estrogen receptor α (ERα; 1:50; Santa Cruz Biotechnology), CK14 (1:50; Santa Cruz Biotechnology), or CK18 (1:40; Santa Cruz Biotechnology) at room temperature overnight. Corresponding secondary FITC-conjugated antibody was applied followed by 4′,6-diamidino-2-phenylindole staining (Molecular Probes). The disks were mounted with Vectashield medium (Vector Laboratories) and images were captured by Zeiss fluorescence microscopy (Zeiss).

Colony formation assay. Single-cell suspensions from mammospheres exposed with or without estrogen were plated on collagen-coated plates at a density of 5,000 viable cells/10-cm-diameter dish as described (10). After 21 d, the colonies were fixed with methanol/acetic acid (3:1) and stained with 0.5% crystal violet solution for 10 min. The size of the colonies was measured and counted. Two-tailed Student's t test was used to assess the significance of the observed differences in colony formation assay.

MeDIP assay and CpG island microarray hybridization. MeDIP was performed on 2 μg sonicated genomic DNA (300–1,000 bp) using a modification of the method described previously (13). Methylated DNA was immunoprecipitated at 4°C overnight with 30 μL of polyclonal antibody against 5-methylcytosine (Abcam). After serial washings, DNA was purified by phenol-chloroform extraction. The immunoprecipitated DNA and input DNA (10 ng) were then ligated to linkers and amplified by linker-mediated PCR as described previously (13). MeDIP-enriched and input DNAs (2 μg) were labeled with Cy5 and Cy3 dyes, respectively (12), and cohybridized to a human CpG island microarray (Agilent Technologies). Oligonucleotide probes (~185,000, 45-mers to 60-mers) were selected to target 27,800 CpG islands (7–24 probes per CpG island; Agilent Technologies). The hybridized slides were scanned by a GenePix 4000B scanner (Axon) and the acquired images were analyzed with GenePix Pro 6.0 (Axon). Dye-swap experiments were conducted, and Lowess-normalized data of duplicated microarray experiments were used to identify significant methylated loci ($P < 0.001$) using a peak detection algorithm in the ChIP Analytics 1.3 software (Agilent). To confirm candidate methylated genes identified by MeDIP-chip, primers targeting the enriched region were designed. PCR was performed with immunoprecipitated or input DNA. Specific primers for amplification are available on request.

Methylation-specific PCR and bisulfite sequencing. DNA was isolated from breast tissues and cell lines using QIAamp DNA Mini kit and 0.5 μg from each sample was treated with sodium bisulfite using EZ DNA Methylation kit (ZYMO Research). Methylation-specific PCR (MSP) primers targeting the MeDIP-enriched regions of *MXI1, RPRM, TFAP2C*, and *WNT5A* genes were designed using Methyl Primer Express Software v1.0 (Applied Biosystems). Primer sequences and conditions for amplification are available on request. The primers used for *RUNX3* have been described previously (14). Amplified products were electrophoresed on 2% agarose gels and visualized with ethidium bromide. For sequencing, bisulfite-treated DNA was amplified using primers for the *RUNX3* promoter region (forward primer, YGGGGTAAATGTTAGAAATTTGT; reverse primer, ACCCCAAAC-TACTTAAAATCCCT). PCR products were cloned into TOPO TA cloning kit (Invitrogen). Five to 10 randomly picked clones were sequenced using ABI 3730 DNA analyzer (Applied Biosystems) and analyzed using the BiQ Analyzer.

Quantitative methylation analysis using MassARRAY. Bisulfite-treated DNA (1 μg) was amplified with specific primers for the *RUNX3* promoter region. MassARRAY platform was used to perform quantitative methylation analysis (Sequenom). This system uses matrix-assisted laser desorption ionization time-of-flight mass spectrometry in combination with RNA base cleavage (MassCLEAVE). Details of quantitative analysis of methylation status have been described elsewhere (15). Two-tailed Student's t test was used to assess the significance of the observed differences in MassARRAY when the averaged methylation ratios of different breast tissue types were compared. Statistical significance was assigned at $P < 0.05$.

5-Aza-2′-deoxycytidine treatment and real-time quantitative RT-PCR. MCF-7 cells were treated with 5 μmol/L 5-aza-2′-deoxycytidine (5-aza-dC) for 5 d in MEM containing 10% FBS and 6 ng/μL insulin. During the final 72 h of 5-aza-dC treatment, cells were hormone deprived by culturing in phenol red–free MEM supplemented with 4% charcoal-dextran–treated FBS. During the final 48 h of hormone deprivation, cells were treated with 1 μmol/L 4-hydroxy-tamoxifen (4-OHT) or vehicle (DMSO) followed by treatment with vehicle (0-h time point) or 10 nmol/L E2 for the indicated time period. RNA (2 μg) was extracted and reverse transcribed with SuperScript III reverse transcriptase (Invitrogen). *RUNX3* mRNA levels were measured using SYBR Green (Applied Biosystems) on a 7500 Real-Time PCR System apparatus. TATA-binding protein (*TBP*) mRNA levels were also measured as a control. Primer sequences and conditions for amplification are available on request.

Gene expression analyses. Total RNA was extracted from microdissected breast tissues [23 invasive ductal carcinomas (IDC), 28 adjacent normal tissues, and 10 reduction mammoplasties], and the quality of RNA samples was assessed using Agilent 2100 Bioanalyzer. Microarray hybridizations were performed by the Core Facility at the Dana-Farber Cancer Institute. The RNA was amplified and labeled according to Affymetrix guidelines and applied to Affymetrix GeneChip Human Genome U133 Plus 2.0 arrays (Affymetrix). The quality of hybridization data was assessed using normalized unscaled SE and relative log expression statistics (16) and MAS5.0 report quality scores. Normalized unscaled SE and relative log expression statistics were computed using the affyPLM package in Bioconductor. Expression values were computed from the raw (.cel) Affymetrix files and normalized using robust multichip averaging RMA (Bioconductor release 2.4.0). Detailed sample histology and clinical information and raw (.cel) and RMA-normalized data for these 61 gene expression profiles are available in ArrayExpress (accession number: E-TABM-276). The gene expression levels of the two Affymetrix probe sets for *RUNX3* (204197_s_at, 204198_s_at) were highly correlated ($r = 0.87$) and were not significantly different ($P > 0.05$, Student's t test). Further analyses of *RUNX3* expression were performed on the mean gene expression level of

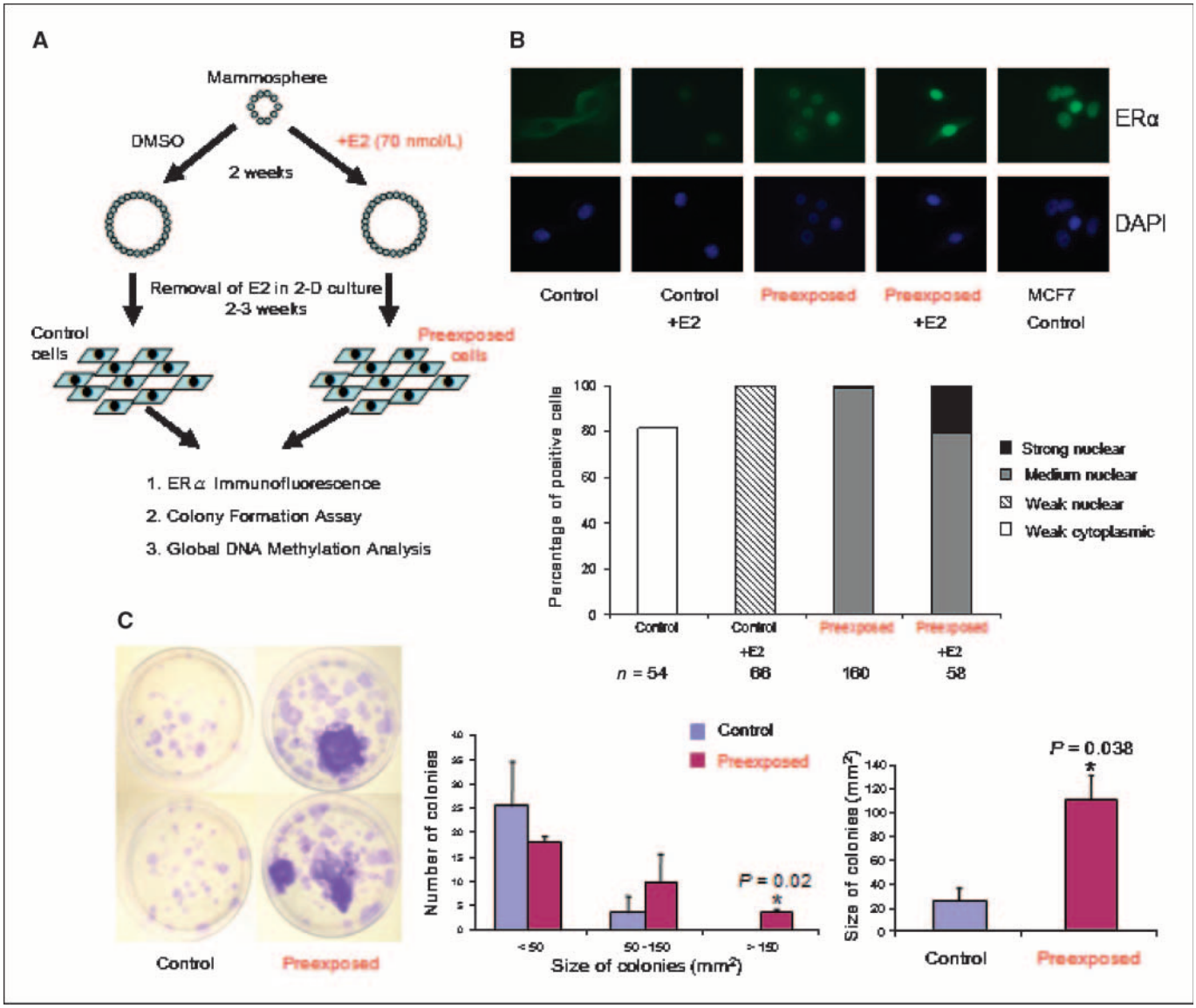

Figure 1. Preexposure of breast progenitor cells to estrogen increases proliferation of progeny epithelial cells. *A,* the breast progenitor cells were propagated as floating spherical colonies, called mammospheres, and treated with 70 nmol/L E2 or DMSO solvent control for 2 wk. To induce differentiation, cells were seeded on a collagen substratum in the absence of E2 for 2 to 3 wk. Phenotypic and epigenetic analyses were then performed on the progeny epithelial cells. *B,* immunofluorescence shows that some progenitor-derived epithelial cells express ERα. After E2 stimulation (10 nmol/L, 3 h), translocation of ERα protein from the cytoplasm and into the nucleus was seen, suggesting functional estrogen signaling. In contrast, epithelial cells preexposed to high-dose estrogen exhibited nuclear ERα localization before E2 stimulation, reminiscent of MCF-7 cells. The percentage, subcellular localization, and staining intensity of ERα-positive cells are shown in the bar chart. The numbers of cells listed in each category were independently scored by two researchers. *C, left,* cell proliferation was measured by colony formation assay. Representative results of two independent experiments are shown. Exposure of progenitor cells to estrogen significantly increased the number of large-sized colonies ($P = 0.02$; *middle*) and the overall size of colonies ($P = 0.038$; *right*) formed by epithelial progeny cells. *Columns,* mean of two independent experiments; *bars,* SD. *Asterisks,* statistical significance.

these two probe sets. One IDC sample (T8703A1) was excluded as outlier in all analyses. To evaluate *RUNX3* expression in breast tissue, we performed a general linear model ANOVA between *RUNX3* gene expression and tissue histology and patient ERα status. To test the association of *RUNX3* and *ESR1* gene expression in breast tissue samples, the Pearson's product-moment correlation coefficient was calculated. Further details, normalized *RUNX3* expression data, and the R code to perform these statistical analyses are available online.[8] *RUNX3* expression levels (RMA-normalized log2 values) derived from Affymetrix microarray experiments of a panel of 51 breast cell lines were also extracted from a recent report (17). Four noncancerous cell lines (HBL100, MCF10A, MCF12A, and SUM190PT) were excluded for analysis. Two-tailed Student's *t* test was used to test if *RUNX3* expression (mean of the two probe sets as described above) was significantly different in breast cancer cell lines according to ERα status. Statistical significance was assigned at $P < 0.05$. Statistically significant results were also obtained when all 51 cell lines were included in the analysis.

Microarray data. The MeDIP-chip microarray data are accessible from the Gene Expression Omnibus (GSE7844). The raw data for expression profiling of human breast tumors and adjacent tissues are available at ArrayExpress (E-TABM-276).

[8] http://compbio.dfci.harvard.edu/publications.html

Supplementary data. The supplementary data include four supplementary figures and one supplementary table.

Results

Estrogen preexposure of breast progenitors alters hormone receptor signaling and promotes clonal proliferation of their epithelial progeny. An *in vitro* protocol has recently been developed to enrich and propagate breast stem and progenitor cells using tissue samples obtained from reduction mammoplasties (10). These cells formed spherical colonies, called mammospheres, in suspension culture. Although a mammosphere may contain progenitor cells that are capable of differentiating into different types of epithelial cells, a subpopulation (<0.1%) of cells with self-renewal ability is believed to be stem cells (10). We independently established this culture method in the laboratory and showed that the isolated mammospheres exhibited the same progenitor characteristics as previously described (see Supplementary Fig. S1).

To investigate whether the model system can be used to simulate an estrogen imprinting event, mammospheres derived from reduction mammoplasties were continuously exposed to E2 (70 nmol/L) or DMSO (control) for 2 weeks (Fig. 1*A*), a treatment scheme known to induce transformation of the human breast epithelial cell line MCF-10F (11). Estrogen treatment stimulated self-renewal of breast progenitors, indicated by a significant increase in the number of mammospheres ($P < 0.01$; Supplementary Fig. S1*A*). After the exposure, E2 was removed from culture dishes, and progenitor cells were placed in fresh hormone-free medium on two-dimensional collagen substratum for 2 to 3 weeks (Fig. 1*A*). Under this two-dimensional culture condition, breast progenitors differentiated into epithelial cells, which were confirmed by immunostaining with epithelial markers (Supplementary Fig. S1*B*).

We then determined whether this estrogen exposure resulted in changes of ERα signaling in progenitor-derived epithelial cells. Immunofluorescence analysis showed that a low level of cytoplasmic ERα was present in 80% of control epithelial cells. Following E2 stimulation (10 nmol/L for 3 h), we observed ERα translocating into the nucleus in some of the differentiated cells (Fig. 1*B*). However, this nuclear localization of ERα before E2 stimulation was already evident in epithelial cells derived from estrogen-exposed progenitors. In addition, stronger nuclear staining of these cells was observed after E2 stimulation, a condition reminiscent to that of receptor-positive breast cancer cells (18). These affected progeny also formed significantly larger colonies and exhibited an increased rate of proliferation compared with the control cells ($P = 0.02–0.038$; Fig. 1*C*). The findings indicate that an imprinting process may occur in breast progenitors preexposed to estrogen, resulting in an alteration of nuclear receptor signaling and clonal expansion in their epithelial progeny.

Estrogen-induced DNA hypermethylation occurs in genes commonly associated with the maintenance of stem and progenitor functions. To determine whether epigenetic processes play a role in this estrogen imprinting, we compared profiles of DNA methylation between estrogen preexposed and control progeny using a methylation screening approach, called MeDIP-chip (13). Methylated DNA, immunoprecipitated with an antibody specific for 5-methylcytosine, and input DNA were labeled with different fluorescent dyes and cohybridized to a microarray panel containing nearly all the annotated human CpG islands ($n = 27,800$). MeDIP-chip analysis in two replicates showed that 0.5% (120 loci) of the CpG islands were hypermethylated in epithelial cells derived from estrogen-exposed progenitors compared with the nonexposed control cells (Supplementary Table S1; Fig. 2*A*). Sequence analysis showed that 111 of these loci are located near the transcription start site (TSS) of genes. Thirteen gene-related loci with diverse MeDIP enrichments were randomly selected for confirmation analyses. Primers flanking the enriched regions were designed for gene-specific PCR assays, and estrogen-induced hypermethylation was confirmed in 92% (12 of 13) of these loci (Fig. 2*B*). Expression analysis of four such loci (*RUNX3, MXI1, RPRM*, and *WNT5A*) further indicates that this hypermethylation event is associated with down-regulation of the corresponding genes (Fig. 2*C*). In addition, MSP was conducted to determine whether the estrogen-induced hypermethylation could be observed in other epithelial cells prepared from different mammoplasties (Fig. 2*D*). Hypermethylation of three loci (*MXI1, TFAP2C*, and *WNT5A*) could be confirmed in some, but not all, epithelial progeny samples, likely attributed to individual variability.

Ontological analysis of the 111 loci revealed significant methylation enrichment of genes related to nucleic acid and cellular metabolism, transcriptional control, and Wnt signaling (Supplementary Fig. S2*A*). Interestingly, 23% ($n = 25$) of these loci are known targets of polycomb proteins that play a role in maintaining pluripotency of stem and progenitor cells (Supplementary Fig. S2*B*; ref. 19). Promoter hypermethylation of polycomb target genes is frequently observed during tumorigenesis (20). Furthermore, eight of the positive loci (*EGR2, FANCF, MXI1, PTPRG, RPRM, RUNX3, TFAP2C*, and *WNT5A*) identified by MeDIP-chip are known tumor suppressor genes, the down-regulation of which was observed in various types of cancer (Supplementary Fig. S2*C*; refs. 14, 21–24). Taken together, our results indicate that key developmental regulators can be epigenetically targeted by estrogen, leading to deregulation of self-renewal of stem and progenitor cells and also tending to promote tumorigenesis.

Estrogen-induced DNA hypermethylation can frequently be seen in primary tumors. To determine whether estrogen-induced methylation changes observed in progenitor-derived epithelial cells also occur in breast tumors, we examined five loci (*MXI1, RPRM, RUNX3, TFAP2C*, and *WNT5A*) in a cohort of breast samples. As indicated earlier, these five loci have previously been reported to be tumor suppressors in different cancer types. MSP analysis was performed on 31 primary tumors, 8 cancer cell lines, and 10 control samples. Hypermethylation of these genes was observed in 23% to 74% of these tumors, but the methylation frequencies (25–100%) were slightly higher in cancer cell lines (Fig. 3). The results are consistent with the previously reported methylation frequencies (37% and 52%) for two genes, *RPRM* and *RUNX3*, in breast tumors (14, 24). In contrast, low methylation frequencies were detected in the reduction controls. The prevalence of these estrogen-induced epigenetic changes in breast tumors therefore provides evidence for a mechanistic basis underlying how promoter CpG islands acquire DNA methylation during cancer development (20).

Estrogen-induced hypermethylation of *RUNX3* can frequently be seen in histologically normal tissue adjacent to the tumor site. We choose *RUNX3*, a developmental transcription factor regulated by polycomb repressors (19), for detailed methylation analysis in histologically normal tissues adjacent to primary tumors. Although inactivation of *RUNX3* is known to play a role in tumorigenesis (14, 25), the mechanism of how this

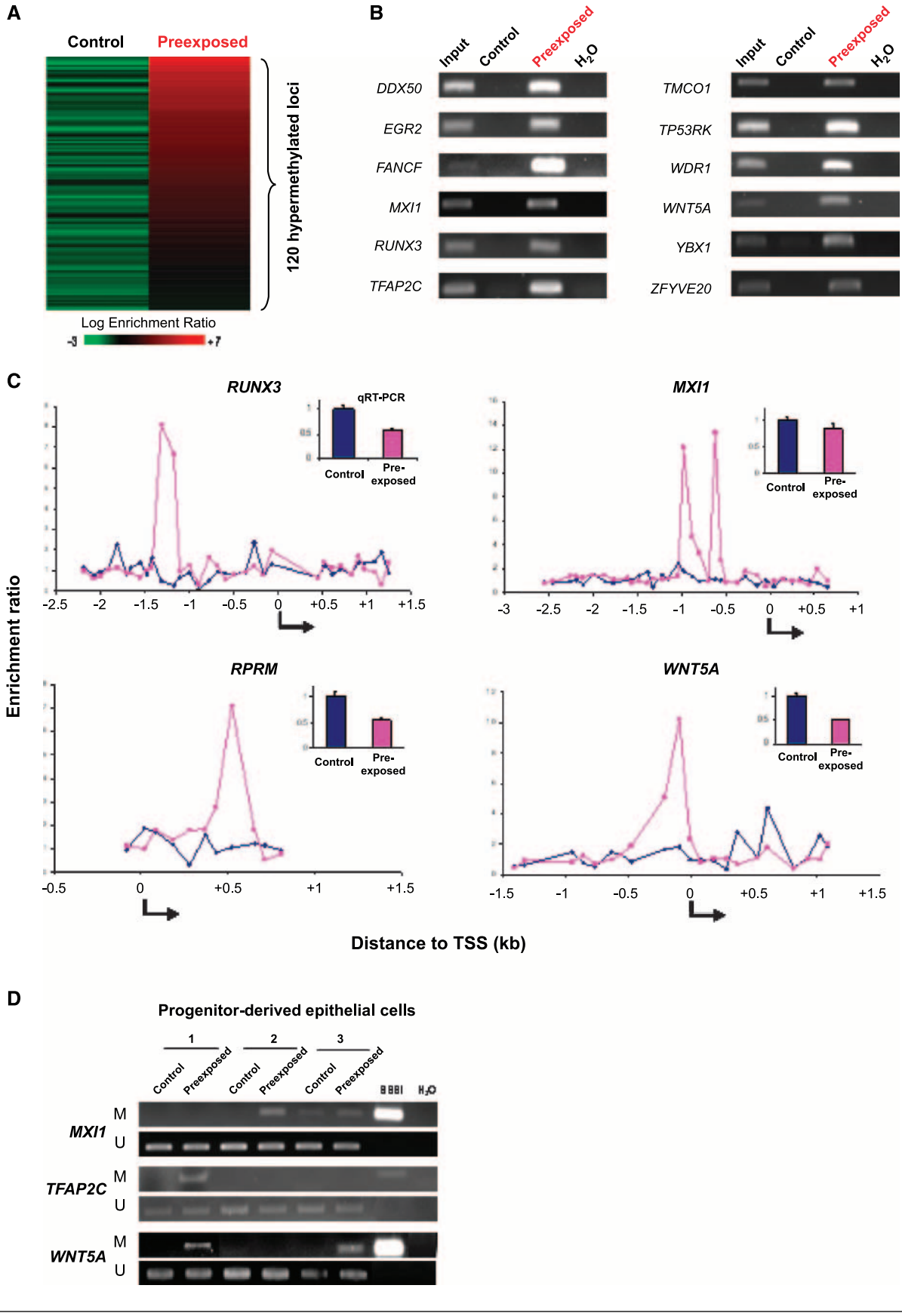

silencing event occurs in early breast tumorigenesis has not been elucidated.

MassARRAY, an assay simultaneously quantifying multiple methylated sites based on their molecular mass (15), was used to determine the methylation status of a 2-kb *RUNX3* promoter region in nine sets of microdissected tumors and adjacent normal tissues (n = 40; Fig. 4*A*). These normal tissues were obtained from four successive zones, each 1 to 4 cm away from the tumor site of the ipsilateral breast (Fig. 5*A, left*). In one case (patient 10486), normal tissues from four quadrants of the contralateral breast were used as controls (Fig. 5*A, right*). In addition, eight unrelated tissues obtained from reduction mammoplasties were included in the analysis.

We observed hypermethylation (e.g., regions 3, 4, and 5) of *RUNX3* in at least five (4993, 9993, 9348, 10486, and 10501) of the nine primary tumor sites (Fig. 4*B*). The overall methylation levels in their corresponding normal tissues (1–4 cm away from tumor sites) also seemed to be higher than those of the eight reduction controls. The boundaries of this hypermethylation were clearly observed at ~0.5 and 1.7 kb upstream of the TSS (Fig. 4*C*). In this regard, methylation levels through this plateau were higher in tumors compared with adjacent normal tissues (P = 0.00038) or reduction controls (P = 0.0027). Notably, methylation levels were higher (P = 1.88e−11) in adjacent normal tissues compared with reduction controls. Bisulfite sequencing and MassARRAY analyses of an overlapping fragment (region 1) yielded concordant results (Fig. 4*D*). At the distal end of the sequencing region, where the beginning of the *RUNX3* methylation plateau was observed by MassARRAY, dense methylation was detected in tumor 4993 and its adjacent normal tissues but not in three reduction controls. In addition, in the first exon region of *RUNX3*, extensive methylation was observed in three tumor pairs and adjacent normal tissues, whereas only a few CpG sites were methylated in reduction normal tissue (Supplementary Fig. S3).

We then performed an in-depth individual gradient analysis using the area with the greatest methylation difference (Fig. 5). Five patient samples with elevated methylation levels in the primary tumor site showed a gradual decrease in DNA methylation with increasing distance up to 4 cm (Fig. 5*B, top*). However, methylation levels in tumors from the other four patients were almost identical to those seen in reduction normal tissues (Fig. 5*B, bottom*). The four quadrant control tissues from the contralateral breast of patient 10486 also exhibited similar basal methylation level. Taken together, these results show that *RUNX3* methylation may precede morphologic transformation of normal breast epithelia in a subset of patients. This observation supports the concept that estrogen-induced hypermethylation in progenitor cells is an early carcinogenic event and may create a large field of cancerization in the human breast.

Epigenetic suppression of *RUNX3* expression is mediated by estrogen signaling in hormone receptor–positive breast cancer. Although underexpression of *RUNX3* frequently occurs in breast cancer compared with normal epithelium (14), the expression of *RUNX3* in histologic normal tissue adjacent to the primary tumor and the relationship between *RUNX3* expression and ERα status have not been investigated. We thus determined mRNA levels of *RUNX3* in a panel of 23 microdissected primary IDC tissues, 28 adjacent normal tissues, and 10 reduction tissues using expression data derived from Affymetrix microarray experiments. *RUNX3* expression in IDC was significantly down-regulated (P < 0.0005) compared with both reduction normal tissues and adjacent normal tissues (Fig. 6*A*), in agreement with a recent report (14). When the tumors were segregated by ERα status, *RUNX3* expression in ERα-positive IDC was significantly lower (P = 0.028) compared with ERα-negative IDC (Fig. 6*B*). Although no difference in overall expression of *RUNX3* was observed in adjacent normal tissues versus reduction normal tissues (Fig. 6*A*), *RUNX3* expression was significantly lower (P = 0.048) in normal breast tissues adjacent to ERα-positive breast tumors versus ERα-negative counterparts (Fig. 6*B*). Overall, a strong negative correlation (r = −0.52; P = 2.51e−5) of *RUNX3* and *ERα* (*ESR1*) gene expression was observed in this set of breast samples (Supplementary Fig. S4). In addition, examination of *RUNX3* expression from an Affymetrix data set of 47 breast cancer cell lines (17) conclusively indicated that *RUNX3* expression was significantly lower (P = 0.0011) in ERα-positive compared with ERα-negative cell lines (Fig. 6*C*). Collectively, the MassARRAY and gene expression analyses show that *RUNX3* expression is inversely correlated with hypermethylation of *RUNX3* and ERα status.

To determine if estrogen signaling plays a role in *RUNX3* silencing, we performed a gene reactivation study using quantitative RT-PCR in ERα-positive MCF-7 breast cancer cells displaying *RUNX3* hypermethylation (Fig. 3*B*). *RUNX3* expression was first reactivated by 5-aza-dC treatment (data not shown); subsequent treatment with E2 resulted in transient down-regulation of *RUNX3* mRNA levels (Fig. 6*D*). Pretreatment with 4-OHT, an ERα antagonist, partially inhibited the E2-induced down-regulation, providing the direct evidence that estrogen suppression of *RUNX3* is, in part, mediated by ERα.

Discussion

Developmental exposure to estrogen and related endocrine disruptors is known to increase breast cancer risk in women (1, 2). As indicated earlier, epidemiologic studies have suggested an imprinting mechanism in which early exposure of environmental estrogens potentiates a carcinogenic process observed later in life

Figure 2. Preexposure of progenitor-derived epithelial cells to estrogen causes DNA hypermethylation and transcriptional silencing of tumor suppressor genes. *A,* differentially methylated genes in estrogen-preexposed progenitor-derived epithelial cells were identified by MeDIP-chip using a microarray panel containing 27,800 CpG islands. The maximum MeDIP enrichment along 120 hypermethylated loci in control and preexposed cells are shown in the heat map (see Supplementary Table S1 for a complete list of the hypermethylated loci). The heat map represents the averaged values of two independent experiments. *B,* to confirm candidate methylated genes determined by microarray, PCR primers targeting the MeDIP-enriched region were designed and the immunoprecipitated control/preexposed DNA samples were amplified along with input DNA. PCRs of no template (H_2O) control are also shown. Twelve of 13 tested genes were validated by PCR analyses. *C,* DNA methylation landscaping maps by plotting the enrichment ratio of each probe of the hypermethylated genes. The preexposed cells (*red line*) displayed an enriched methylated region of multiple probes, within the CpG island, located in proximity to the TSS (*arrow*); no significant enrichment was observed in control cells (*blue line*). Genes showing DNA hypermethylation in preexposed cells were associated with transcriptional suppression [shown by real-time quantitative RT-PCR (*qRT-PCR*); *upper right, inset*]. *Columns,* mean of three independent experiments; *bars,* SD. *D,* methylation status of tumor suppressor gene promoter regions was confirmed by MSP in control/preexposed DNA samples derived from three individuals. MSP PCR primers targeting MeDIP-enriched regions were designed. Preexposed cells of at least one set of samples showed DNA methylation in these tumor suppressor genes. *M,* PCR product with primers specific for methylated genes; *U,* unmethylated genes.

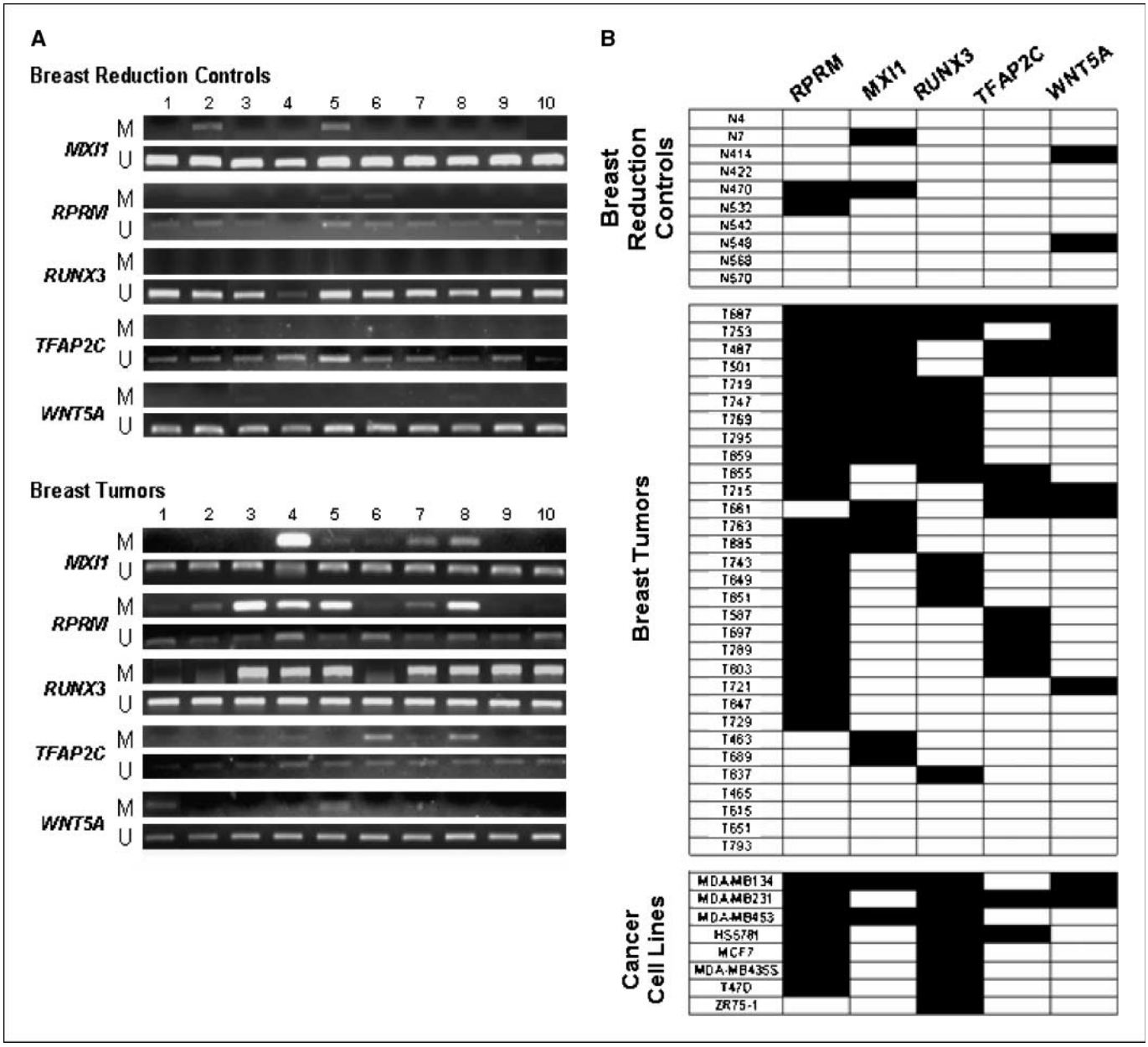

Figure 3. Estrogen-induced hypermethylation of tumor suppressor loci is also present in breast tumors. *A,* MSP analyses for tumor suppressor gene promoter methylation in breast reduction normal tissues (*top*) and primary tumors (*bottom*). Representative gel pictures show data for 10 of a total of 31 tumor tissues examined and 10 breast reduction normal tissues. *B,* summary of methylation data for all tissue samples and cancer cell lines. Aberrant methylation of these tumor suppressor genes occurred in a high percentage of primary tumors (23–74%) and cancer cell lines (25–100%) compared with reduction normal controls (0–20%).

(1, 3). In the past, it is difficult to study how this imprinting mechanism is operated at the molecular level. Presently, we show that mammospheres, which contain enriched breast stem and progenitor cells (10), can be a model system for this type of study. Our rationale is that long-lived, slow-growing breast progenitors are more susceptible to environmental injuries than terminally differentiated epithelial cells, which have a high turnover rate in the breast duct. With this prior notion, we designed the experiment by exposing mammospheres to estrogen (i.e., E2) and later completely removed E2 from the culture medium and allowed breast progenitors to undergo epithelial differentiation in two-dimensional collagen stratum.

Although the mammosphere model system cannot exactly imitate a real-life scenario, the experimental design is useful to determine whether an imprinting phenomenon could be recreated *in vitro*. The E2 dose (70 nmol/L) used in the present study is higher than typically seen in women under normal physiologic conditions or having prior history of estrogen exposure. In a previous study by Russo et al. (11), they found that, at this dose of treatment, estrogen caused cellular transformation of a breast epithelial cell line, MCF-10F. When transformed cells with aggressive behavior were further filtered through an invasion chamber, these clonal cells could grow into tumors in a xenograft model. Unlike MCF-10F, our primary epithelial cells derived from

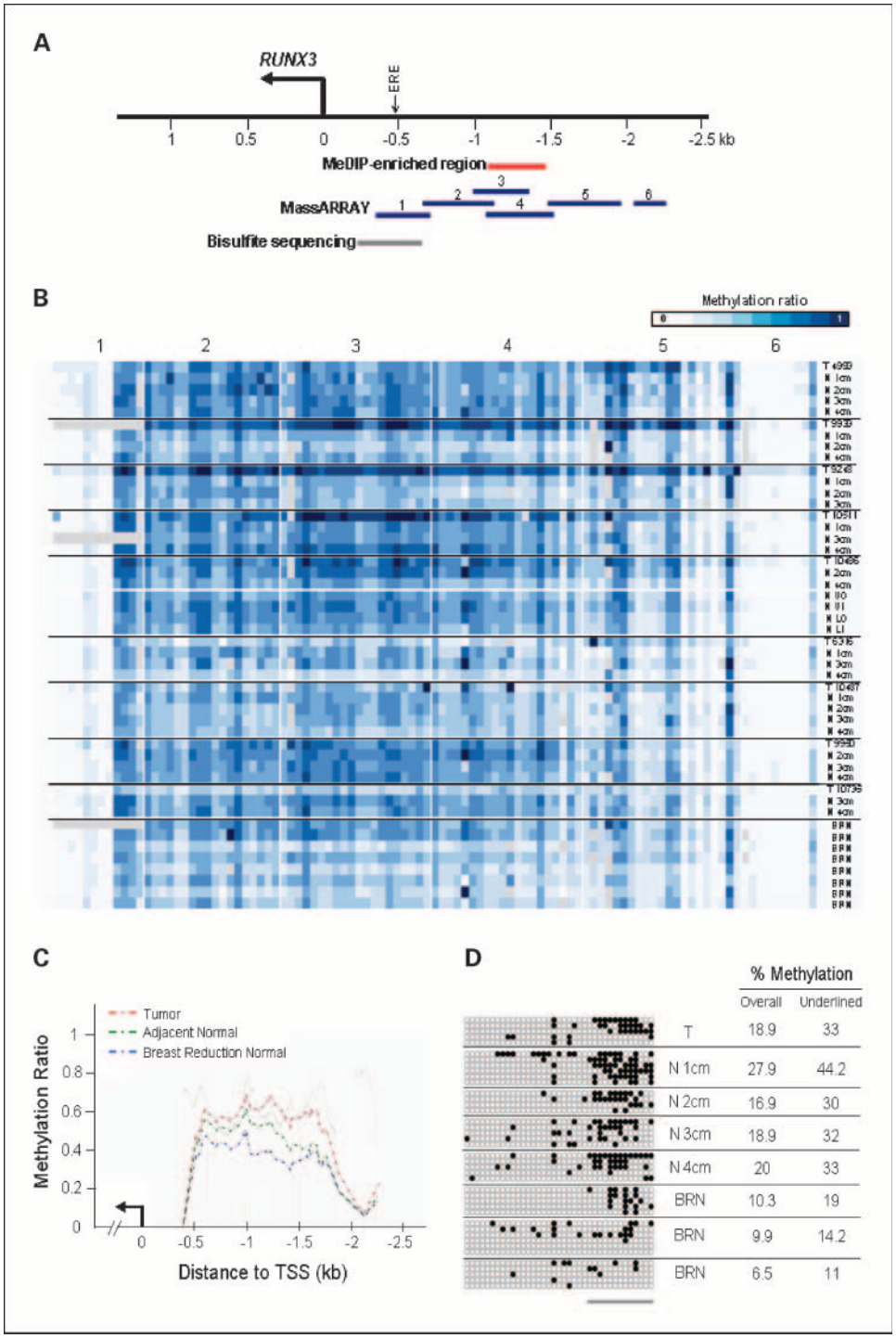

Figure 4. DNA hypermethylation of *RUNX3* in breast tumors and adjacent histologically normal tissues. *A,* genomic map of the *RUNX3* promoter CpG island. *Arrow, RUNX3* TSS in the genome sequence; *inverted arrow,* potential estrogen-responsive element (*ERE*; predicted by MATCH using the TRANSFAC database). *Red bar,* MeDIP-enriched region. Locations of the *RUNX3* promoter fragments interrogated by MassARRAY (*blue bars*) and bisulfite sequencing (*gray bar*). *B,* quantitative methylation results from MassARRAY analysis of *RUNX3* promoter region in primary breast tissues. Six amplicons covering a total of 101 CpG sites, located approximately 0.3 to 2.3 kb upstream of the *RUNX3* TSS, were designed to analyze 9 sets of breast tumor (*T*)/adjacent normal (*N*) tissues and 8 breast reduction normal tissues (*BRN*; 48 samples total). CpG site measurements in the analyzed region of the *RUNX3* promoter for all samples are depicted in the heat map. *Blue color intensity,* methylation ratios (see scale bar); *gray,* missing data values. Each row represents methylation data from one tissue sample. Tissues from each cancer patient are separated by black lines. Each column (spaced by white lines) represents methylation data from each amplicon. *C,* summation of the overall methylation levels of each tissue type in a genomic context. *Red dotted lines,* methylation ratios of tumor tissues; *green dotted lines,* methylation ratios of adjacent normal tissues; *blue dotted lines,* methylation ratios of breast reduction normal tissues; *gray lines,* CpG content in the amplification region calculated for a moving 100-bp window. *D,* bisulfite sequencing analysis of *RUNX3* promoter region in one set of breast tumor/adjacent normal tissues and three breast reduction normal tissues. *Black dots,* methylated CpG sites; *white dots,* unmethylated sites. The underlined region is near the beginning of the methylation plateau observed by MassARRAY. The percentages of CpG methylation of the overall and underlined regions are indicated for each tissue. Breast tumor and adjacent histologically normal tissues showed significantly higher methylation levels compared with breast reduction normal tissues, in agreement with the MassARRAY analysis. Additional bisulfite sequencing results are shown in Supplementary Fig. S3.

estrogen-treated progenitors did not produce tumors in female athymic mice after 6 months of transplantation (data not shown). Additional molecular alterations need to be acquired in these primary epithelial cells to increase their tumorigenic potential. Future studies can also be performed to test tumorigenicity of different doses of estrogen and other endocrine disruptors using this mammosphere system.

There are limitations in this mammosphere model system. Genetic variations and other confounding factors (e.g., menopausal status and age) may affect estrogenic susceptibility of individuals. Therefore, we could not anticipate concordant results when different breast progenitor samples are exposed to the same dose of estrogen (see Fig. 2*D*). The experimental findings derived from this study may be biased toward patients undergoing breast reduction procedures. Ethically, we could not obtain breast tissue samples from healthy individuals with a known exposure history of endocrine disruptors. Nevertheless, the model system proposed here represents a new paradigm, simulating a condition of early breast carcinogenesis that is associated with exposure to environmental estrogen. We have shown that estrogen exposure stimulates self-renewal of breast progenitors (Supplementary Fig. S1*A*) and increases proliferation of the derived epithelial progeny (Fig. 1*C*), both of which are associated with alterations in the methylome. Because such epigenetic alterations were not observed in the differentiated epithelial cells *in vitro* (Fig. 2) and *in vivo* (Fig. 3), we strongly contend that the methylation changes

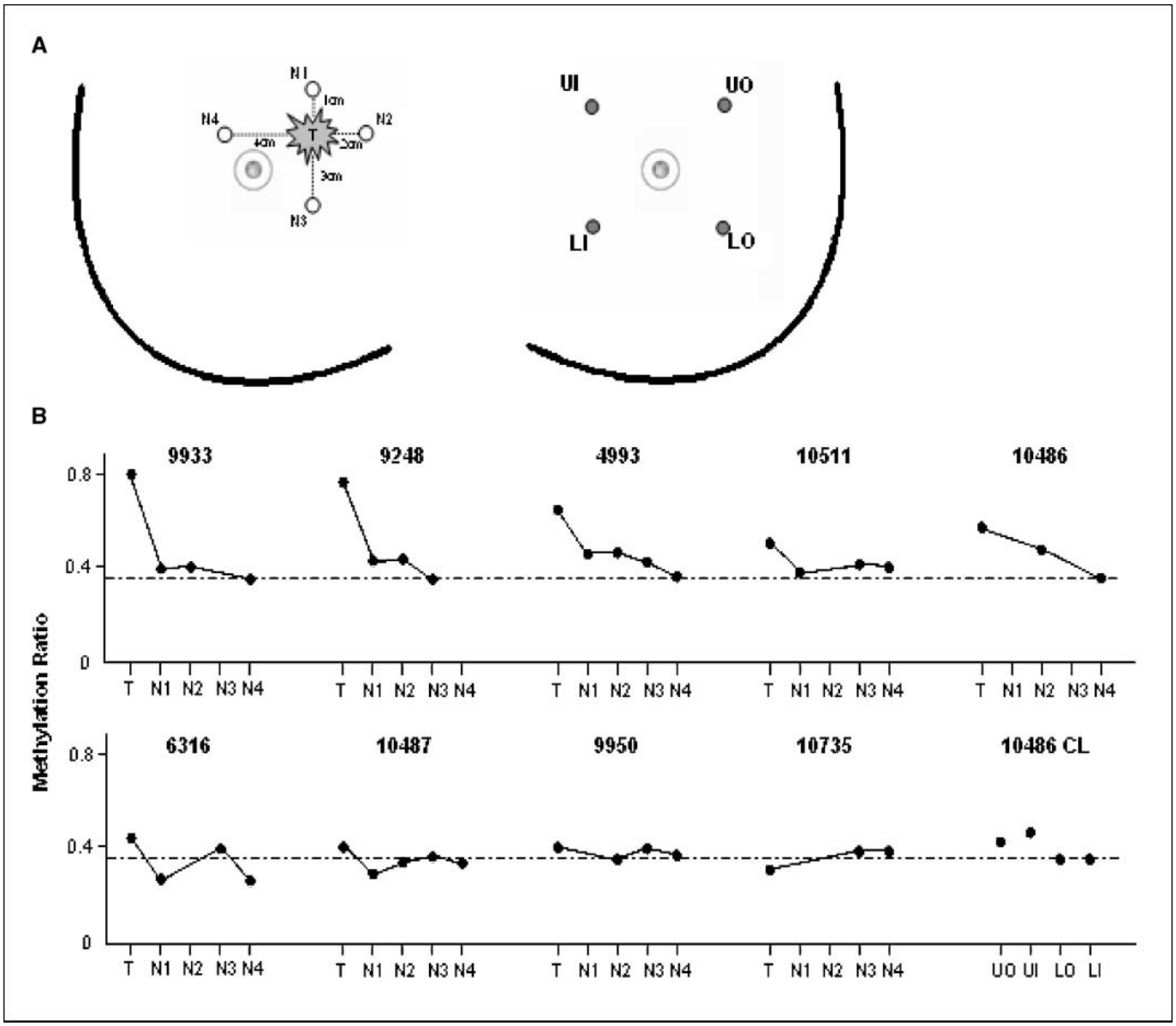

Figure 5. Mapping geographic zones of *RUNX3* DNA methylation in histologically normal tissues adjacent to breast tumor. *A,* microdissected breast tissues from patients undergoing mastectomy were collected. Mastectomy specimens were marked for tumor and its surrounding zones N1 (1 cm), N2 (2 cm), N3 (3 cm), and N4 (4 cm) from the grossly visible tumor boundary. In bilateral and prophylactic mastectomy cases, normal breast tissues were taken from the four quadrants of the breast. *UO,* upper outer; *UI,* upper inner; *LO,* lower outer; *LI,* lower inner. *B,* the graphs show methylation ratios of the primary breast tumor and adjacent normal tissues of indicated distance (cm) from tumor boundary of each patient. Data of contralateral (*CL*) prophylactic mastectomy normal epithelia of patient 10486 are also shown. *Dotted lines,* mean methylation ratio for breast reduction normal tissues as reference.

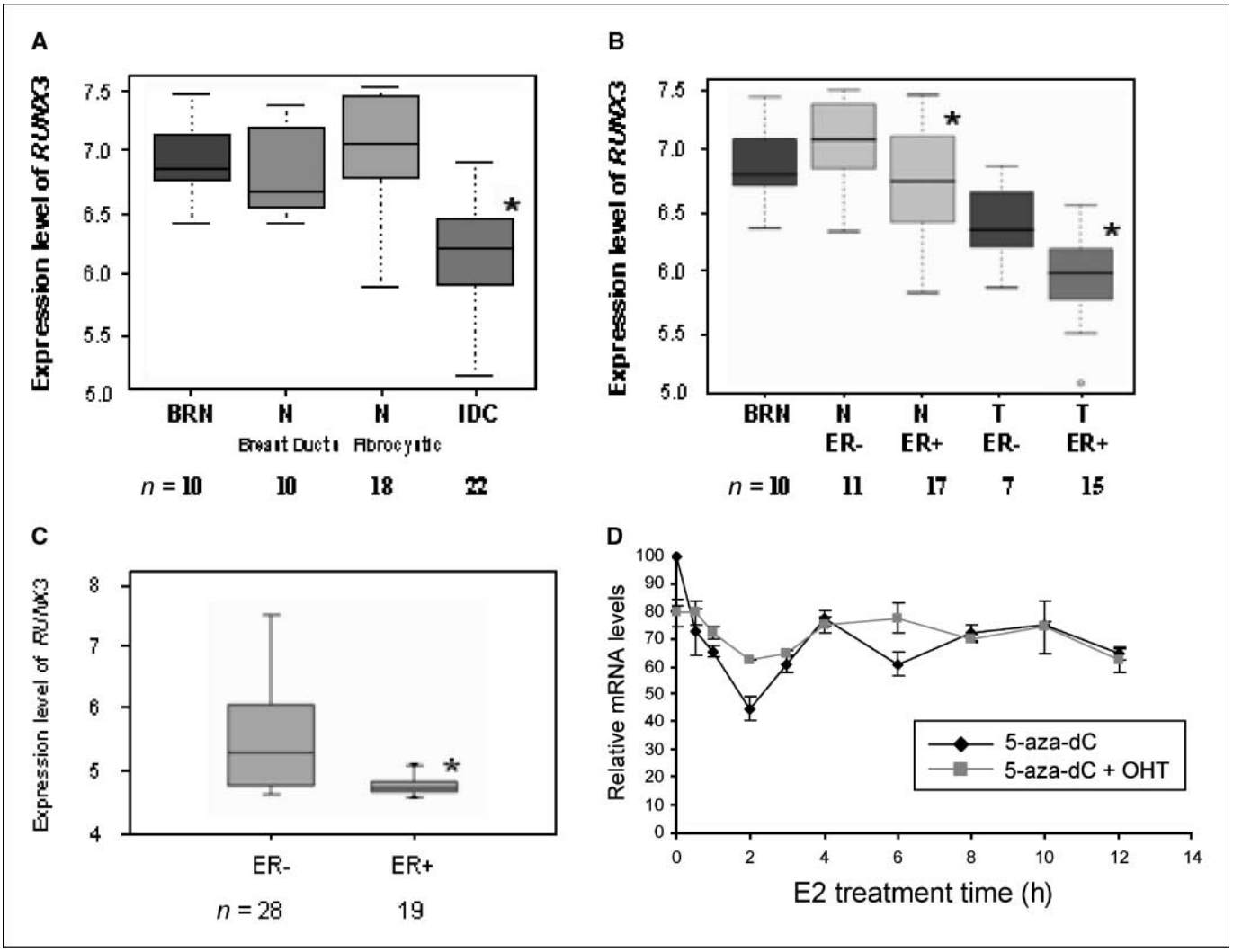

Figure 6. Inverse correlation between *RUNX3* expression and ERα status. *A, RUNX3* mRNA expression was significantly lower in IDC tissues compared with breast reduction normal tissues. No difference in *RUNX3* expression was observed in adjacent normal tissues with unremarkable breast ducts and fibrocystic/nonproliferative changes versus reduction normal tissues. *B,* ERα-positive IDC had significantly reduced *RUNX3* mRNA expression compared with ERα-negative tumors. Notably, normal breast tissues adjacent to ERα-positive breast tumors also had significantly lower expression than ERα-negative counterparts. *C,* evaluation of *RUNX3* mRNA expression in a panel of breast cancer cell lines. ERα-positive cell lines had significantly lower *RUNX3* expression than ERα-negative cell lines, in agreement with the data from primary breast tissues. In *A* to *C*, expression levels are represented in log2 values. In the box plots, the upper and lower boundaries of the box indicate 75th and 25th percentiles, respectively. *Line within the box,* median; *bars above and below the box,* 90th and 10th percentiles, respectively. The numbers of tissues/cell lines studied are also indicated. *Asterisks,* statistical significance. *D,* real-time quantitative RT-PCR analysis of *RUNX3* in MCF-7 cells after a 5-d treatment with 5 μmol/L 5-aza-dC. *Black line,* 5-aza-dC–treated MCF-7 cells were hormone deprived for 72 h and treated with vehicle or 10 nmol/L E2 for the indicated times (h); *gray line,* 5-aza-dC–treated and hormone-deprived cells were treated with 4-OHT (1 μmol/L for 48 h) and then treated with vehicle or 10 nmol/L E2 for the indicated times (h). Results are presented relative to no 4-OHT treatment control (*black line*, 0 time point). *Points,* mean of triplicates; *bars,* SD.

were not a consequence of cell differentiation. Alternatively, we propose that estrogen induces epigenetic alterations in breast progenitors leading to mammary carcinogenesis.

Our proof-of-principle study shows that critical genes controlling tumor suppression, such as *RUNX3*, can be down-regulated on estrogen exposure to breast progenitors. Recent reports have shown that breast progenitor cells express ERα (26, 27). Thus, the down-regulation may be mediated, in part, by the canonical pathway of estrogen signaling (see Fig. 6*D*). This finding is also supported by the presence of nuclear ERα in the affected epithelial progeny; this nuclear internalization is commonly seen in hormone receptor–positive breast cancer with functional estrogen signaling (18). As reported in our previous study (12), estrogen can induce H3K9 dimethylation, a repressive chromatin modification (28), and transiently suppresses a set of ERα-responsive genes in breast cancer cells. The presence of dimethyl H3K9 mark may promote a repressive mode that renders target genes more vulnerable to long-term silencing during cancer development (29). Based on existing reports and our present study, we propose that progressive accumulation of DNA methylation plays a final role in both maintaining permanent silencing of tumor suppressor genes and transmitting this heritable information from breast progenitors to their epithelial progeny. Although our MeDIP data only provide methylation information of the affected epithelial progeny, a sensitive immunoprecipitation technique (30) can be implemented in the

future to directly interrogate the methylome of mammospheres containing only 2,000 to 10,000 cells. Comparing the methylomes between the hormone-treated mammospheres and their derived epithelial progeny will lead to better understanding of the estrogen epigenetic imprinting phenomenon.

Although the present study reports estrogen-induced hypermethylation, we also observed preferential MeDIP enrichment of ~0.5% of CpG island loci analyzed in the control epithelial progeny relative to those of the affected progeny (data not shown). This could be a hypomethylation event, which may require a functional demethylase yet to be characterized in the affected progeny. Hypomethylation of non-CpG islands is known to occur in repeat sequences of the cancer genome (6). Because our microarray panel contains only single-copy CpG islands, the issue of whether estrogen induces hypomethylation of repeat sequences during epithelial differentiation remains to be explored. One more plausible explanation is that promoter methylation of these CpG islands occurs during normal maturation of particular epithelial branches in the breast duct. It is possible that, as a result of estrogen exposure, these promoter CpG islands escape methylation-mediated silencing, and subsequent activation of the corresponding genes may promote clonal proliferation of the affected epithelial progeny. Future research direction will require isolation of primary epithelial cells from different lineages by flow cytometry using defined surface markers and separately analyze their methylomes by MeDIP-chip. These challenging studies will determine whether the estrogen treatment can induce a true hypomethylation event or prevent an epigenetically mediated maturation process in the affected progeny.

In conclusion, the mammosphere model described in this study may provide a new paradigm for assessing cancer risk due to exposure to endocrine disruptors. The *in vitro* system may serve as a viable alternative to animal models and other toxicologic assays for testing new estrogenic compounds. Furthermore, the altered methylome cataloged in this study can be used to identify biomarkers for early breast cancer detection and biosensors for environmental estrogens.

Acknowledgments

Received 9/20/2007; revised 12/18/2007; accepted 1/22/2008.

Grant support: NIH grants U54 CA11300, R01 CA069065, P30 CA16058, and R01 CA098522 and U01 ES015986; The Ohio State University Comprehensive Cancer Center; and Li Ka Shing Institute of Health Sciences.

The costs of publication of this article were defrayed in part by the payment of page charges. This article must therefore be hereby marked *advertisement* in accordance with 18 U.S.C. Section 1734 solely to indicate this fact.

We thank Dr. Jose Russo (Fox Chase Cancer Center) for advice on estrogen treatment scheme and Chieh-Ti Kuo, Enrica Fabbri, Sandya Liyanarachchi, Daniel Deatherage, and Huaxia Qin (Ohio State University) for technical support.

References

1. Fenton SE. Endocrine-disrupting compounds and mammary gland development: early exposure and later life consequences. Endocrinology 2006;147:S18–24.
2. Yager JD, Davidson NE. Estrogen carcinogenesis in breast cancer. N Engl J Med 2006;354:270–82.
3. Ho SM, Tang WY, Belmonte de Frausto J, Prins GS. Developmental exposure to estradiol and bisphenol A increases susceptibility to prostate carcinogenesis and epigenetically regulates phosphodiesterase type 4 variant 4. Cancer Res 2006;66:5624–32.
4. Newbold RR, Padilla-Banks E, Jefferson WN. Adverse effects of the model environmental estrogen diethylstilbestrol are transmitted to subsequent generations. Endocrinology 2006;147:S11–7.
5. Robertson KD. DNA methylation and human disease. Nat Rev Genet 2005;6:597–610.
6. Jones PA, Baylin SB. The fundamental role of epigenetic events in cancer. Nat Rev Genet 2002;3:415–28.
7. Weissman IL, Anderson DJ, Gage F. Stem and progenitor cells: origins, phenotypes, lineage commitments, and transdifferentiations. Annu Rev Cell Dev Biol 2001;17:387–403.
8. Feinberg AP. Methylation meets genomics. Nat Genet 2001;27:9–10.
9. Yan PS, Venkataramu C, Ibrahim A, et al. Mapping geographic zones of cancer risk with epigenetic biomarkers in normal breast tissue. Clin Cancer Res 2006;12:6626–36.
10. Dontu G, Abdallah WM, Foley JM, et al. *In vitro* propagation and transcriptional profiling of human mammary stem/progenitor cells. Genes Dev 2003;17:1253–70.
11. Russo J, Fernandez SV, Russo PA, et al. 17-β-Estradiol induces transformation and tumorigenesis in human breast epithelial cells. FASEB J 2006;20:1622–34.
12. Cheng AS, Jin VX, Fan M, et al. Combinatorial analysis of transcription factor partners reveals recruitment of c-MYC to estrogen receptor-α responsive promoters. Mol Cell 2006;21:393–404.
13. Weber M, Davies JJ, Wittig D, et al. Chromosome-wide and promoter-specific analyses identify sites of differential DNA methylation in normal and transformed human cells. Nat Genet 2005;37:853–62.
14. Lau QC, Raja E, Salto-Tellez M, et al. RUNX3 is frequently inactivated by dual mechanisms of protein mislocalization and promoter hypermethylation in breast cancer. Cancer Res 2006;66:6512–20.
15. Ehrich M, Nelson MR, Stanssens P, et al. Quantitative high-throughput analysis of DNA methylation patterns by base-specific cleavage and mass spectrometry. Proc Natl Acad Sci USA 2005;102:15785–90.
16. Bolstad BM, Collin F, Brettschneider J, et al. Quality assessment of Affymetrix GeneChip data. In: Gentleman R, Carey V, Huber W, Irizarry R, Dudoit S, editors. Bioinformatics and computational biology solutions using R and Bioconductor. New York: Springer. 2005. p. 33–47.
17. Neve RM, Chin K, Fridlyand J, et al. A collection of breast cancer cell lines for the study of functionally distinct cancer subtypes. Cancer Cell 2006;10:515–27.
18. Stenoien DL, Patel K, Mancini MG, et al. FRAP reveals that mobility of oestrogen receptor-α is ligand- and proteasome-dependent. Nat Cell Biol 2001;3:15–23.
19. Lee TI, Jenner RG, Boyer LA, et al. Control of developmental regulators by Polycomb in human embryonic stem cells. Cell 2006;125:301–13.
20. Widschwendter M, Fiegl H, Egle D, et al. Epigenetic stem cell signature in cancer. Nat Genet 2007;39:157–8.
21. Kremenevskaja N, von Wasielewski R, Rao AS, Schöfl C, Andersson T, Brabant G. Wnt-5a has tumor suppressor activity in thyroid carcinoma. Oncogene 2005;24:2144–54.
22. McPherson LA, Loktev AV, Weigel RJ. Tumor suppressor activity of AP2α mediated through a direct interaction with p53. J Biol Chem 2002;277:45028–33.
23. Schreiber-Agus N, Meng Y, Hoang T, et al. Role of Mxi1 in ageing organ systems and the regulation of normal and neoplastic growth. Nature 1998;393:483–7.
24. Takahashi T, Suzuki M, Shigematsu H, et al. Aberrant methylation of Reprimo in human malignancies. Int J Cancer 2005;115:503–10.
25. Fukamachi H. Runx3 controls growth and differentiation of gastric epithelial cells in mammals. Dev Growth Differ 2006;48:1–13.
26. Clarke RB, Spence K, Anderson E, Howell A, Okano H, Potten CS. A putative human breast stem cell population is enriched for steroid receptor-positive cells. Dev Biol 2005;277:443–56.
27. Woodward WA, Chen MS, Behbod F, Rosen JM. On mammary stem cells. J Cell Sci 2005;118:3585–94.
28. Barski A, Cuddapah S, Cui K, et al. High-resolution profiling of histone methylations in the human genome. Cell 2007;129:823–37.
29. Ohm JE, McGarvey KM, Yu X, et al. A stem cell-like chromatin pattern may predispose tumor suppressor genes to DNA hypermethylation and heritable silencing. Nat Genet 2007;39:237–42.
30. O'Neill LP, VerMilyea MD, Turner BM. Epigenetic characterization of the early embryo with a chromatin immunoprecipitation protocol applicable to small cell populations. Nat Genet 2006;38:835–41.

Epithelial Progeny of Estrogen-Exposed Breast Progenitor Cells Display a Cancer-like Methylome

Alfred S.L. Cheng, Aedín C. Culhane, Michael W.Y. Chan, et al.

Cancer Res 2008;68:1786-1796.